



# Revisiting a skeleton model for the mammalian cell cycle: From bistability to Cdk oscillations and cellular heterogeneity<sup>☆</sup>

Claude Gérard<sup>1</sup>, Didier Gonze, Albert Goldbeter<sup>\*</sup>

Unité de Chronobiologie théorique, Faculté des Sciences, Université Libre de Bruxelles (ULB), Campus Plaine, CP 231, B-1050 Brussels, Belgium



## ARTICLE INFO

### Article history:

Received 21 June 2018

Revised 16 October 2018

Accepted 19 October 2018

Available online 21 October 2018

## ABSTRACT

A network of cyclin-dependent kinases (Cdks) regulated by multiple negative and positive feedback loops controls progression in the mammalian cell cycle. We previously proposed a detailed computational model for this network, which consists of four coupled Cdk modules. Both this detailed model and a reduced, skeleton version show that the Cdk network is capable of temporal self-organization in the form of sustained Cdk oscillations, which correspond to the orderly progression along the different cell cycle phases G1, S (DNA replication), G2 and M (mitosis). We use the skeleton model to revisit the role of positive feedback (PF) loops on the dynamics of the mammalian cell cycle by showing that the multiplicity of PF loops extends the range of bistability in the isolated Cdk modules controlling the G1/S and G2/M transitions. Resorting to stochastic simulations we show that, through their effect on the range of bistability, multiple PF loops enhance the robustness of Cdk oscillations with respect to molecular noise. The model predicts that a rise in the total level of Cdk1 also enlarges the domain of bistability in the isolated Cdk modules as well as the range of oscillations in the full Cdk network. Surprisingly, stochastic simulations indicate that Cdk1 overexpression reduces the robustness of Cdk oscillations towards molecular noise; this result is due to the increased distance between the two branches of the bistable switch at higher levels of Cdk1. At intermediate levels of growth factor stochastic simulations show that cells may randomly switch between cell cycle arrest and cell proliferation, as a consequence of fluctuations. In the presence of Cdk1 overexpression, these transitions occur even at low levels of growth factor. Extending stochastic simulations from single cells to cell populations suggests that stochastic switches between cell cycle arrest and proliferation may provide a source of heterogeneity in a cell population, as observed in cancer cells characterized by Cdk1 overexpression.

© 2018 Elsevier Ltd. All rights reserved.

## 1. Introduction

In mammalian cells the series of biochemical processes leading from one cell division to the next, constituting the cell cycle, is controlled by a set of enzymatic reactions. A network of enzymes known as cyclin-dependent kinases (Cdks) drives the orderly progression along the four successive phases of the mammalian cell cycle, namely G1, S (DNA replication), G2, and M (mitosis) (Morgan, 1995). If cells do not proliferate, they remain in a quiescent state, or enter into a program of cell differentiation. The Cdk network is regulated by a variety of intertwined negative and positive feedback loops. Negative feedback loops play a key

role in generating self-sustained oscillations in the Cdk network, as shown initially for the early cell cycles in amphibian embryos (Felix et al., 1990; Goldbeter, 1991, 1996; Tyson, 1991). A number of experimental and theoretical studies, mostly devoted to the cell cycle in amphibian embryos (Novak and Tyson, 1993; Sha et al., 2003; Vinod et al., 2013) and to the yeast cell cycle (Barik et al., 2010; Chen et al., 2004; Novak and Tyson, 1997), showed that positive feedbacks contribute, through eliciting bistability, to the robustness of oscillatory behavior. In particular, multiple positive feedback loops are at the core of the regulatory mechanisms driving the G1/S and G2/M transitions (Dirick and Nasmyth, 1991; Ferrell et al., 2009; He et al., 2011; Holt et al., 2008; Kapuy et al., 2009; Novak et al., 2007; Pomerening et al., 2005; Sha et al., 2003; Skotheim et al., 2008; Swat et al., 2004; Tyson and Novak, 2001). These positive feedbacks trigger all-or-none cyclin/Cdk activation, which allows for irreversible transitions between two successive cell cycle phases.

We previously proposed a detailed computational model for the dynamics of the Cdk network driving the mammalian cell cycle

<sup>☆</sup> This article is further included in a [special issue of JTB dedicated to the memory of Prof. René THOMAS](#).

<sup>\*</sup> Corresponding author.

E-mail address: [agoldbet@ulb.ac.be](mailto:agoldbet@ulb.ac.be) (A. Goldbeter).

<sup>1</sup> Current address: de Duve Institute, Université catholique de Louvain (UCL), Avenue Hippocrate 75, B-1200 Brussels, Belgium

(Gérard and Goldbeter, 2009; Gérard and Goldbeter, 2011; Gérard and Goldbeter, 2014; Gérard et al., 2012), as well as a simpler, skeleton model containing a reduced number of variables, which reproduces the dynamic behavior of the full model for the Cdk network. In both models, which consist of four coupled cyclin/Cdk modules, the increase in growth factor above a critical value elicits the transition from a stable steady state, corresponding to cell cycle arrest, to sustained Cdk oscillations associated with cell proliferation (Gérard and Goldbeter, 2009; Gérard and Goldbeter, 2011; Gérard and Goldbeter, 2014). Using the skeleton model we previously showed that multiple positive feedback (PF) loops enhance the robustness of Cdk oscillations with respect to molecular noise (Gérard et al., 2012). Here we examine in further detail how positive feedback loops shape the dynamics of the Cdk network and enhance the robustness of oscillatory behavior.

Examining the role of multiple positive feedback loops on the dynamics of the mammalian cell cycle seems appropriate in an issue of the *Journal of Theoretical Biology* dedicated to the memory of René Thomas. Indeed, René Thomas contributed for long to clarify the conditions in which positive regulatory circuits give rise to multiple steady states, the best known example of which is bistability, i.e. the coexistence of two stable steady states (Thomas, 1978; Thomas and d'Ari, 1990; Thomas et al., 1995; Thomas and Kaufman, 2001). As indicated above, positive feedback is encountered repeatedly in the Cdk network that governs the cell cycle, so that the conditions for bistability are met in multiple ways within this regulatory network (Dirick and Nasmyth, 1991; Ferrell et al., 2009; Gonze and Hafner, 2010; He et al., 2011; Holt et al., 2008; Kapuy et al., 2009; Novak et al., 2007; Pomerening et al., 2005; Sha et al., 2003; Skotheim et al., 2008; Swat et al., 2004; Tyson and Novak, 2001).

Our previous results, based on stochastic simulations, indicated that multiple PF loops enhance the robustness of Cdk oscillations by extending the range of bistability in the isolated Cdk modules controlling the G1/S and G2/M transitions. While an increase in the level of the cyclin-dependent kinase Cdk1, involved in the G2/M transition, also extends the range of bistability, we report the counterintuitive result that such an extended range can in fact be accompanied by a decrease in the robustness of Cdk oscillations with respect to molecular noise. We assess the effect of fluctuations on the random switching between quiescence and proliferation in single cells. Extending stochastic simulations from single cells to cell populations suggests that such switches between cell cycle arrest and proliferation, triggered by fluctuations, may provide a source of heterogeneity in a cell population, as observed in cancer cells characterized by high levels of Cdk1.

## 2. Detailed and skeleton models for the Cdk network

The detailed model describing the dynamics of the Cdk network driving the mammalian cell cycle consists of four Cdk modules, each centered around one cyclin/Cdk complex (Gérard and Goldbeter, 2009). Cyclin D/Cdk4-6 and cyclin E/Cdk2 promote progression in G1 and elicit the G1/S transition, respectively; cyclin A/Cdk2 ensures progression in S and the transition S/G2, while the activity of cyclin B/Cdk1 brings about the G2/M transition. This detailed model for the Cdk network contains 39 variables, and includes both negative and positive feedback loops. We used this model to show that in the presence of sufficient amounts of growth factor the Cdk network is capable of temporal self-organization in the form of sustained oscillations (Gérard and Goldbeter, 2009). The latter correspond to the repetitive, ordered, sequential activation of the various cyclin/Cdk complexes that govern the transitions between successive phases of the cell cycle.

In the detailed model for the Cdk network, the activity of cyclin/Cdk complexes is regulated in multiple ways (Gérard and Goldbeter, 2009). In particular, several positive feedback loops characterize the activation of the cyclin-dependent kinases, because the phosphatases Cdc25 that activate various Cdks are themselves activated through phosphorylation by the Cdks (Hoffmann et al., 1993; Goldbeter, 1993), while the latter inactivate their inhibitory kinase Wee1 (Harvey et al., 2005; Harvey et al., 2011).

Relinquishing many of these biochemical details but retaining the essence of the regulatory wiring diagram, we subsequently built a skeleton, 5-variable model for the mammalian cell cycle, which possesses the same dynamical properties as the more detailed model for the Cdk network (Gérard and Goldbeter, 2011). Thus, sustained oscillations in the various cyclin/Cdk complexes occur in the skeleton model in the presence of sufficient amounts of growth factor. The skeleton model also accounts for the existence of a restriction point in G1 beyond which the presence of growth factor is not needed to complete a cycle.

In a first version of the skeleton model we did not incorporate the regulation of Cdk1 and Cdk2 through phosphorylation-dephosphorylation (Gérard and Goldbeter, 2011). In a second step, we extended the skeleton model by incorporating the regulation of Cdk2 and Cdk1 by the phosphatase Cdc25 and the kinase Wee1 (Gérard et al., 2012). This allows us to assess the role of positive feedback on the dynamics of the Cdk network by comparing four situations: (i) no positive feedback (PF) occurs in the network, (ii) a single positive feedback occurs in the second Cdk module of the network, as a result of the self-activation of cyclin E/Cdk2 via its activation of Cdc25, (iii) in addition to this positive regulation of cyclin E/Cdk2, self-activation of cyclin B/Cdk1 occurs through its activation of Cdc25, and (iv) a second positive feedback on Cdk1 occurs through inhibition of Wee1 by cyclin B/Cdk1. This comparative study allowed us to determine the effect of multiple positive feedback loops on the dynamics of the cell cycle (Gérard et al., 2012). In particular, we assessed the role of the apparent redundancy in self-amplification of the Cdk1 module through simultaneous activation of the phosphatase Cdc25 and inhibition of the kinase Wee1.

The skeleton model for the Cdk network is schematized in Fig. 1. At the beginning of the cell cycle, the growth factor GF activates directly the synthesis of the cyclin D/Cdk4-6 complex, which promotes progression in G1. This complex ensures the activation of the transcription factor E2F, which in turn activates the synthesis of the cyclin E/Cdk2 and cyclin A/Cdk2 complexes. During the G1 phase, cyclin E/Cdk2 reinforces the activation of the transcription factor E2F. During S phase, cyclin A/Cdk2 activates the degradation of cyclin E/Cdk2, which ensures that the latter complex will not be active at the end of the cell cycle. Cyclin A/Cdk2 also permits exit of the S phase by allowing the inactivation of the transcription factor E2F and by promoting the synthesis of cyclin B/Cdk1, whose peak of activity brings about the G2/M transition. During mitosis, cyclin B/Cdk1 activates, by phosphorylation, the protein Cdc20. This protein is at the core of two negative feedback loops as it promotes the inactivation of both cyclin A/Cdk2 and cyclin B/Cdk1, thereby permitting completion of the cell cycle. A new cell cycle starts if growth factor is still present in sufficient amount.

The detailed and skeleton models provide us with complementary tools to investigate the emergent dynamical properties of the Cdk network controlling the mammalian cell cycle. While the more detailed version allows us to test the effect of inhibiting or over-expressing a large number of antagonistic factors that control the network, the skeleton version is more amenable to stochastic simulations which are used to assess the robustness of Cdk oscillations with respect to molecular noise.

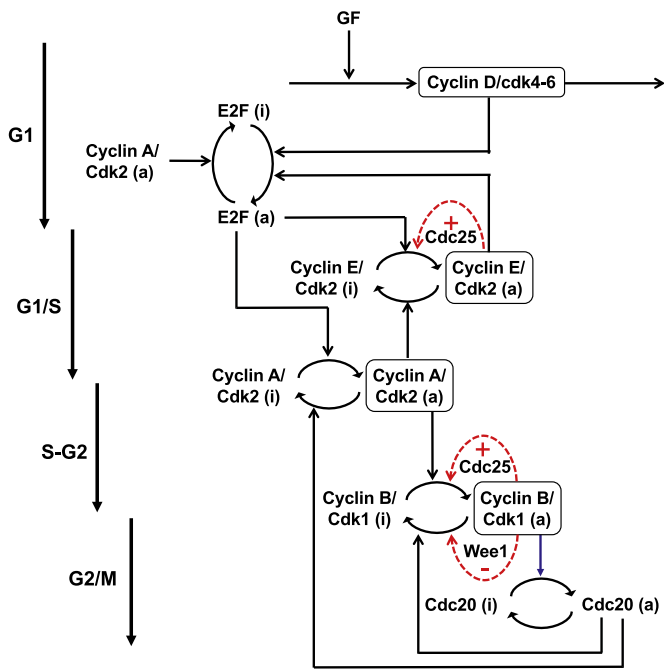


**Fig. 1.** Scheme of the skeleton model for the Cdk network driving the mammalian cell cycle. This model (Gérard et al., 2012) provides a simplified picture of a more detailed model for the Cdk network based on a similar regulatory structure (see text, and Gérard and Goldbeter, 2009). Growth factors (GF) induce synthesis of cyclin D/cdk4-6, which promotes entry into G1. Cyclin D/cdk4-6 and cyclin E/cdk2 activate the transcription factor E2F, which, in its turn, activates cyclin E/cdk2 and cyclin A/cdk2, thereby ensuring progression in S and G2. In G2, cyclin A/cdk2 inhibits E2F and cyclin E/cdk2, thus ensuring a transient, cell-phase specific activation of these factors; cyclin A/cdk2 also activates cyclin B/cdk1, which elicits the G2/M transition. During mitosis, cyclin B/cdk1 activates the protein Cdc20 which targets cyclin A/cdk2 and cyclin B/cdk1 for degradation. For simplicity these degradation processes are modeled here by an inhibition of cyclin A/cdk2 and cyclin B/cdk1. The model includes regulation of Cdk activity by the phosphatases Cdc25 and the kinase Wee1: Cdc25 phosphatases activate by dephosphorylation the various cyclin/Cdk complexes which, in turn, activate the phosphatases by phosphorylation; moreover, the kinases Wee1 and Cdk1 mutually inhibit each other by phosphorylation. For more details, see (Gérard et al., 2012) and Supporting Information where the kinetic equations and parameter values are listed in Tables S1 and S2, respectively.

### 3. Dynamics of the mammalian cell cycle at a single cell level

The qualitative dynamical behavior of the Cdk network in the detailed and the skeleton model is highly similar. Indeed, below a critical level of growth factor (GF), the Cdk network in both models tends to a stable steady state defined by low levels of the various cyclin/Cdk complexes; this steady state can be associated with cell cycle arrest (Fig. 2A, B). In contrast, in the presence of supra-threshold amounts of GF, the Cdk network displays sustained oscillations of the limit cycle type in the levels of various cyclin/Cdk complexes; such sustained Cdk oscillations can be associated with cell proliferation (Fig. 2C, D). In both detailed and skeleton models, the ordered activation of the various cyclin/Cdk complexes ensures a correct progression along the different phases of the mammalian cell cycle.

The regulatory structure of the Cdk network in the two models is similar, and can give rise in both cases to endoreplication (Edgar et al., 2014; Gérard and Goldbeter, 2009; Gérard and Goldbeter, 2010). Endoreplication is defined by the decoupling between DNA replication and mitosis: cells undergo multiple rounds of DNA replication, characterized by sustained oscillations of Cdk2, without entering into mitosis, owing to the reduced level of cyclin B/cdk1 (Fig. 2E, F). Endoreplication leads to polyploidization, which is very frequent in plants and insects (Zielke et al., 2011), and less com-

mon in animals, although it is observed in physiological conditions in some tissues in mammals, such as liver, heart, bone marrow and placenta (Gentric and Desdouets, 2014).

Qualitatively, the temporal dynamics of the cyclin/Cdk complexes in both models is very similar. This shows that the core regulatory structure of the Cdk network suffices to account for the evolution of the network toward sustained oscillations or a stable steady state.

### 4. Positive feedback loops, bistability, and oscillations in the Cdk network

In view of its relative simplicity, the skeleton model for the mammalian cell cycle is well suited to analyze the effect of positive feedback loops on the dynamics of the network (Gérard et al., 2012). Here we extend this study and focus on the G2/M transition of the network, controlled by the cyclin B/cdk1 complex. Steady-state levels of cyclin B/cdk1 as a function of its input, the level of cyclin A/cdk2 considered as a parameter, are shown in the presence of 1 PF loop through Cdc25 (Fig. 3A), 1 PF through Wee1 (Fig. 3C) and 2 PF loops through Cdc25 and Wee1 (Fig. 3E). The results indicate that the presence of PF loops gives rise to bistability in the level of cyclin B/cdk1. Such bistability is associated to a robust G2/M transition: while a low level of cyclin B/cdk1 characterizes the G2 phase, a high level of cyclin B/cdk1 characterizes mitosis. In addition, increasing the number of PF loops enlarges the domain of bistability (compare Figs. 3A and 3C with Fig. 3E). In a two-parameter bifurcation diagram defined by the total levels of cyclin B/cdk1,  $M_{\text{BTOT}}$ , and the active form of cyclin A/cdk2,  $Ma$ , the model exhibits a domain of monostability and a domain of bistability in the level of cyclin B/cdk1 (see Figs. 3B, 3D, 3F). These stability diagrams further illustrate the enlargement of the domain of bistability in presence of multiple PF loops. Horizontal dashed lines in Fig. 3B, D, F correspond to the conditions in Fig. 3A, C, E, respectively.

The two-parameter bifurcation diagrams indicate that the size of the domain of bistability depends on the total level of cyclin B/cdk1,  $M_{\text{BTOT}}$ . Indeed, by plotting the steady-state levels of cyclin B/cdk1 as a function of cyclin A/cdk2 for  $M_{\text{BTOT}} = 1$  (Fig. 4A), 2 (Fig. 4C) and 10 (Fig. 4E) in the presence of 1 PF loop through Wee1, 1 PF loop through Cdc25, or 2 PF loops through both Cdc25 and Wee1, the model shows that an increase in the level of  $M_{\text{BTOT}}$  considerably enlarges the domain of bistability defining the dynamics of the fourth Cdk module, at the core of the G2/M transition (compare Fig. 4A and 4C with 4E).

In Fig. 4, bistability corresponds to an S-shaped curve when plotting cyclin B/cdk1 at steady state as a function of cyclin A/cdk2 (Fig. 4A, C, E). The domain of bistability is bounded by two limit points corresponding to saddle-node bifurcations. On the lower branch, associated to a low level of cyclin B/cdk1, above a critical value of cyclin A/cdk2 (see limit point LP1 in Fig. 4E) we observe a sharp transition to the upper branch corresponding to a higher level of cyclin B/cdk1. Then, upon decreasing the level of cyclin A/cdk2 below a lower critical value (see limit point LP2 in Fig. 4E) we observe a sharp transition back to the lower branch of steady state. It is interesting to note that the position of LP1 does not change much when the total amount of cyclin B/cdk1 ( $M_{\text{BTOT}}$ ) increases. By contrast, LP2 moves to lower and lower values of cyclin A/cdk2 when  $M_{\text{BTOT}}$  increases. This observation can be explained intuitively as follows: on the lower branch, at low values of cyclin B/cdk1, the level of cyclin A/cdk2 must increase up to a critical value (LP1) above which cyclin B/cdk1 reaches a critical level above which the positive feedback triggers a transition to a high steady state of cyclin B/cdk1. This critical level of cyclin A/cdk2 is largely independent of  $M_{\text{BTOT}}$ . On the upper branch, LP2 represents the value below which cyclin A/cdk2 must decrease before cyclin

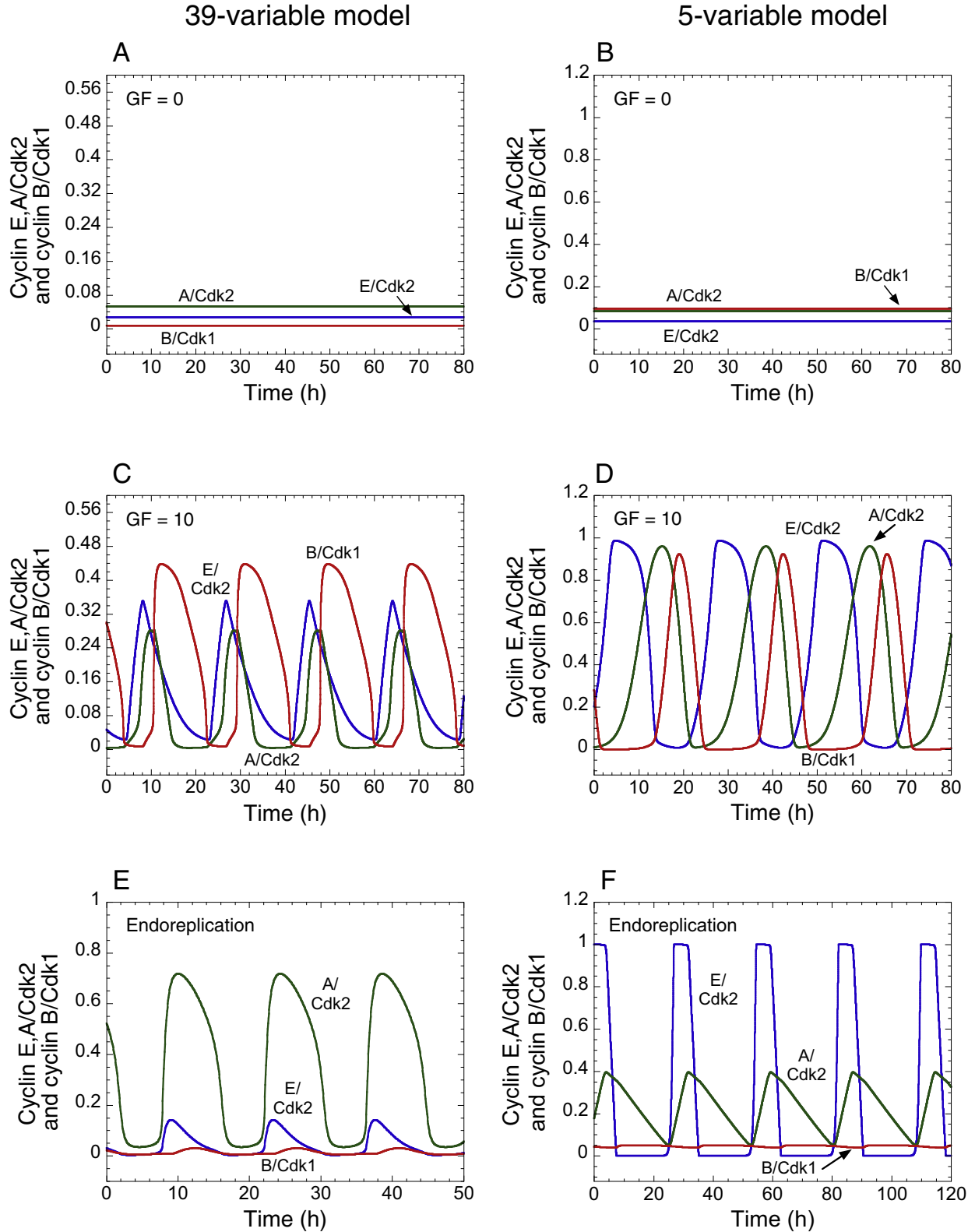


**Fig. 2.** Oscillatory dynamics of the Cdk network in the detailed and skeleton models for the mammalian cell cycle. The time evolution of cyclin E/Cdk2 (blue curve), cyclin A/Cdk2 (green curve) and cyclin B/Cdk1 (red curve) is shown in the detailed, 39-variable, model (A, C, E) and the skeleton, 5-variable, model (B, D, F) in the absence of GF (GF=0 in A and B) or presence of GF (GF=10 nM in C and D), as well as in conditions of endoreplication (E and F). Parameter values are as in (Gérard and Goldbeter, 2009) in A and C. Conditions for E are as in (Gérard and Goldbeter, 2009) with  $V_{S1P27} = 1.2 \text{ nM h}^{-1}$  and  $V_{2CDH1} = 2 \text{ h}^{-1}$ . (B, D) Parameter values are as in Table S2 in Supplementary Information. (F) Conditions are as in Table S2 with  $b_1 = b_2 = 1$ ,  $K_{Ib} = 1000 \text{ nM}$ ,  $K_M = 0.005 \text{ nM}$ ,  $V_{1E2F} = 15 \text{ h}^{-1}$ ,  $V_{2E2F} = 50 \text{ h}^{-1}$ ,  $V_{1ME} = 1.5 \text{ nM}^{-1} \text{ h}^{-1}$ ,  $V_{2ME} = 2 \text{ h}^{-1}$ ,  $V_{1MA} = 0.2 \text{ h}^{-1}$ ,  $V_{2MA} = 10 \text{ h}^{-1}$ ,  $V_{1MB} = 0.1 \text{ nM}^{-1} \text{ h}^{-1}$ ,  $V_{2MB} = 0.9 \text{ h}^{-1}$ ,  $M_{BTOT} = 0.05 \text{ nM}$ ,  $V_{1CDC20} = 3 \text{ h}^{-1}$ ,  $V_{2CDC20} = 0.3 \text{ nM h}^{-1}$ ,  $CDC20_{TOT} = 10 \text{ nM}$ .

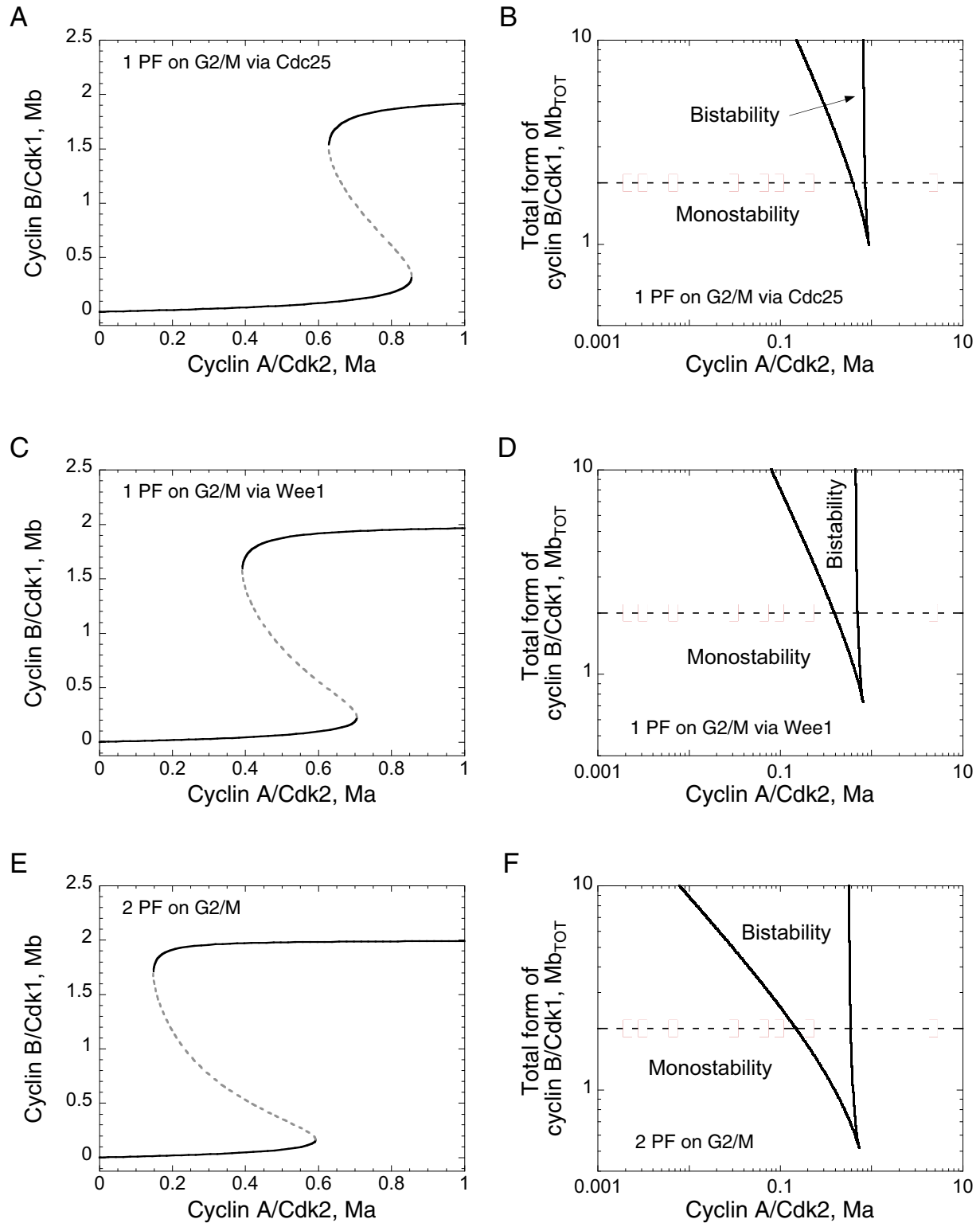


**Fig. 3.** Bistability resulting from positive feedback (PF) in the G2/M transition. Steady-state levels of cyclin B/Cdk1 are plotted as a function of cyclin A/Cdk2, considered as a parameter, in the presence of 1 PF on G2/M through Cdc25 (A), 1 PF on G2/M through Wee1 (C) or 2 PF loops through Cdc25 and Wee1 (E). The dynamical behavior of the G2/M module is represented in a 2-parameter space defined by the total form of cyclin B/Cdk1,  $M_{B,TOT}$ , and the active form of cyclin A/Cdk2,  $Ma$ , for 1 PF on G2/M through Cdc25 (B) or Wee1 (D), or 2 PF loops on G2/M through Cdc25 and Wee1 (F). The size of the domain of bistability increases with the number of PF loops. Horizontal dashed lines in B, D, F correspond to the sections represented in A, C, E, respectively. Parameter values are as in Table S2 with  $K_M = 0.1$  nM,  $\epsilon_{ps} = 0.8$ ,  $V_{1MB} = 0.5$  nM<sup>-1</sup>.h<sup>-1</sup> and  $V_{2MB} = 0.7$  h<sup>-1</sup>. To construct the bifurcation diagram for the Cdk1 module as a function of cyclin A/Cdk2, we disconnected cyclin B/Cdk1 from the rest of the Cdk network and considered only the kinetic equation of cyclin B/Cdk1 ( $M_B$ ), from which we removed  $CDC20$ .

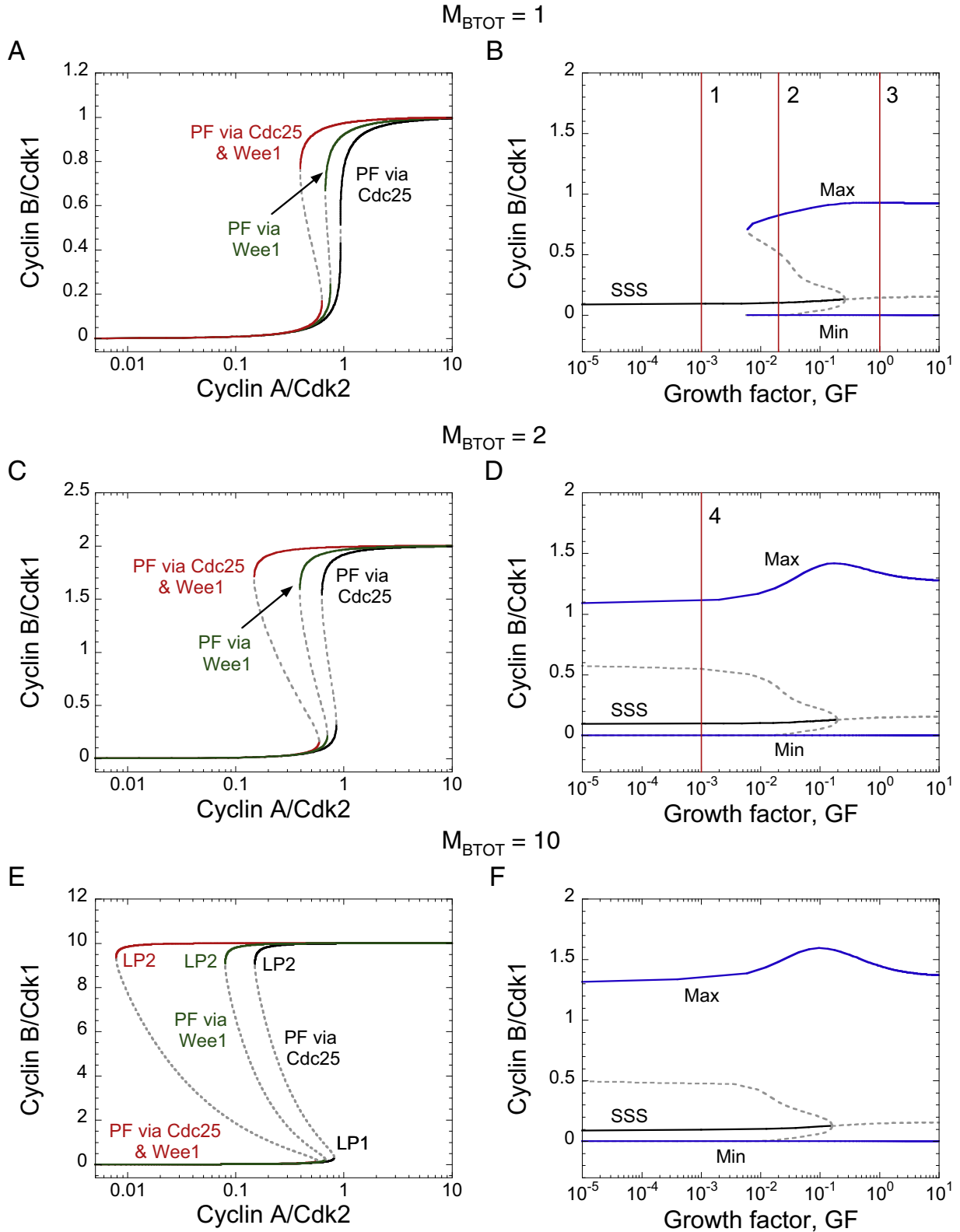


**Fig. 4.** The bistable switch in G2/M and the oscillatory behavior of the Cdk network are controlled by the total cyclin B/Cdk1 level,  $M_{BTOT}$ . Steady-state levels of cyclin B/Cdk1 are plotted as a function of cyclin A/Cdk2 (A, C, E) or as a function of growth factor, GF (B, D, F) for  $M_{BTOT} = 1$  nM (A, B), 2 nM (C, D) and 10 nM (E, F). In A, C, E, the steady-state levels are determined in the presence of 1 PF loop on G2/M through Cdc25 (black curve with  $b_2 = 1$  and  $K_{IB} = 1000$  nM), 1 PF loop via Wee1 (green curve with  $b_2 = 0$  and  $K_{IB} = 0.5$  nM), or 2 PF loops through Cdc25 and Wee1 (red curve with  $b_2 = 1$  and  $K_{IB} = 0.5$  nM). In B, D, F, the steady-state levels are shown with 1 PF loop on G1/S ( $b_1 = 1$ ) and 2 PF loops on G2/M ( $b_2 = 1$  and  $K_{IB} = 0.5$  nM). (A – F) Solid lines: Stable steady states (SSS) or envelope defined by minima (Min) and maxima (Max) reached in the course of the oscillations. Dotted lines: unstable steady states or Min/Max of the unstable limit cycle. Other parameter values are as in Table S2 in Supplementary Information. The vertical lines marked 1–3 in (B) and 4 in (D) refer to conditions considered for stochastic simulations in Figs. 8 and 9.

B/Cdk1 jumps back to a low value once the positive feedback loop involving cyclin B/Cdk1 becomes ineffective. That LP2 diminishes when  $M_{\text{BTOT}}$  increases is due to the fact that less cyclin A/Cdk2 is needed to fuel the positive feedback.

As illustrated by plotting the steady-state levels of cyclin B/Cdk1 as a function of the level of growth factor, GF (Fig. 4B, 4D, 4F), numerical simulations predict that an increase in the total level of cyclin B/Cdk1,  $M_{\text{BTOT}}$ , enlarges the domain of oscillatory behavior of the Cdk network. For  $M_{\text{BTOT}} = 1$  (Fig. 4B), the Cdk network is characterized, for low levels of GF, by a stable steady state corresponding to cell cycle arrest. Sustained oscillations of the Cdk network only occur at suprathreshold levels of GF. Interestingly, for intermediate levels of GF, due to a subcritical Hopf bifurcation, we observe a region of coexistence between a stable steady state and a sustained oscillatory behavior of the Cdk network. This means that for the same GF levels, a cell could be either in a resting (stable steady state) or a proliferative state (sustained oscillatory regime). For larger levels of  $M_{\text{BTOT}}$ , the model predicts such coexistence between a stable steady state and a sustained oscillatory regime (referred to as *hard excitation*) even at low levels of GF (Fig. 4D and 4F). Thus the model indicates that the cell does not depend on GF to proliferate in the presence of an overexpression of  $M_{\text{BTOT}}$ . This result holds with experimental observations which show that cancer cells often overexpress the various cyclins and Cdks, as compared to healthy tissues, and do not require the presence of growth factor to grow (Goustin et al., 1986; Hanahan and Weinberg, 2011). Thus the total level of cyclin B/Cdk1 controls the size of the bistable domain at the core of the G2/M transition as well as the oscillatory properties of the Cdk network, e.g. the occurrence of hard excitation and the dependence of oscillations on the presence of growth factor.

## 5. Stochastic version of the skeleton model for the Cdk network

Molecular noise can arise in cells as a consequence of the low number of mRNA and protein molecules. Stochastic simulations allow to account for this source of variability (Gonze et al., 2018) and to study its effect on the dynamics of the cell cycle. In a previous study (Gérard et al., 2012), we showed by means of stochastic simulations of the skeleton model that the robustness of Cdk oscillations towards molecular noise increases with the number of PF loops in the Cdk network. This conclusion was based on the observation that the range in which bistability occurs increases with the number of PF loops. Stochastic simulations are performed by means of the Gillespie algorithm (Gillespie, 1977). The number of molecules present can be controlled through parameter  $\Omega$  measuring the number of molecules. As  $\Omega$  progressively increases, the trajectories tend to the solution predicted by the deterministic system (see further details about stochastic simulations in Supplementary Information).

To illustrate the impact of PF loops on the robustness of Cdk oscillations, we plot the deterministic (solid thick black line) and stochastic (grey line) limit cycle trajectories projected onto the phase plane (cyclin B/Cdk1 versus cyclin A/Cdk2) in the presence of 1 PF loop on G1/S and 1 PF loop on G2/M (Fig. 5A), 2 PF loops on G2/M (Fig. 5C) and 3 PF loops (1 on G1/S and 2 on G2/M) (Fig. 5E). The corresponding stochastic temporal evolutions of cyclin B/Cdk1 are illustrated in Fig. 5B, D, F, respectively. The model indicates that beyond providing redundancy, PF loop on the G2/M transition is important to increase the robustness of the Cdk oscillations (compare Fig. 5C and D with Fig. 5A and B). Adding PF loops on G1/S transition further increases the robustness of the cell cycle dynamics against molecular noise (compare Fig. 5E and F with Fig. 5C and D).

Such results have been already emphasized in previous theoretical studies (Gérard et al., 2012; Gérard et al., 2015; Gonze and Hafner, 2010; He et al., 2011) and corroborate experimental observations about the role of PF loops for the robustness of the Cdk network dynamics driving progression in the cell cycle (Ferrell et al., 2009; Holt et al., 2008; Kapuy et al., 2009; Pomerening et al., 2005; Skotheim et al., 2008; Tsai et al., 2008).

Since an increase in the total level of cyclin B/Cdk1,  $M_{\text{BTOT}}$ , enlarges the domain of bistability in the activity of cyclin B/Cdk1 (see Figs. 4A, C, E), as well as the domain of sustained oscillatory behavior of the Cdk network (Fig. 4B, D, F), the question arises as to whether the robustness of Cdk oscillations could be improved by modulating the total level of cyclin B/Cdk1. To address this question, we performed deterministic and stochastic simulations in the presence of low ( $M_{\text{BTOT}} = 1$  in Figs. 6A, D, G), intermediate ( $M_{\text{BTOT}} = 2$  in Figs. 6B, E, H) and high levels of  $M_{\text{BTOT}}$  ( $M_{\text{BTOT}} = 10$  in Figs. 6C, F, I). The model predicts that an increase in  $M_{\text{BTOT}}$  will not be accompanied by a strong increase in the level of activity of cyclin B/Cdk1, as illustrated by the deterministic time evolution of cyclin E/Cdk2, cyclin A/Cdk2 and cyclin B/Cdk1 in Fig. 6A, B, C). As a consequence, even if the domain of bistability is larger when  $M_{\text{BTOT}}$  increases, the level of activity of cyclin B/Cdk1 will never reach the upper branch of stable steady state of cyclin B/Cdk1 when  $M_{\text{BTOT}} = 2$  or  $M_{\text{BTOT}} = 10$  (compare the deterministic limit cycle trajectories illustrated by the red curves in Fig. 6E and 6F with Fig. 6D). By superimposing the stochastic limit cycle trajectories on these bifurcation diagrams, we notice that Cdk oscillations are more robust in the presence of low  $M_{\text{BTOT}}$  levels (compare Fig. 6G where  $M_{\text{BTOT}} = 1$  with Fig. 6H and 6I where  $M_{\text{BTOT}} = 2$  and 10, respectively). This is due to the fact that only at the lower value of  $M_{\text{BTOT}}$  does the system reach the upper branch of stable steady state, which provides a buffer with respect to fluctuations since the system has a reduced propensity to jump back to the lower branch of stable steady state in the presence of fluctuations.

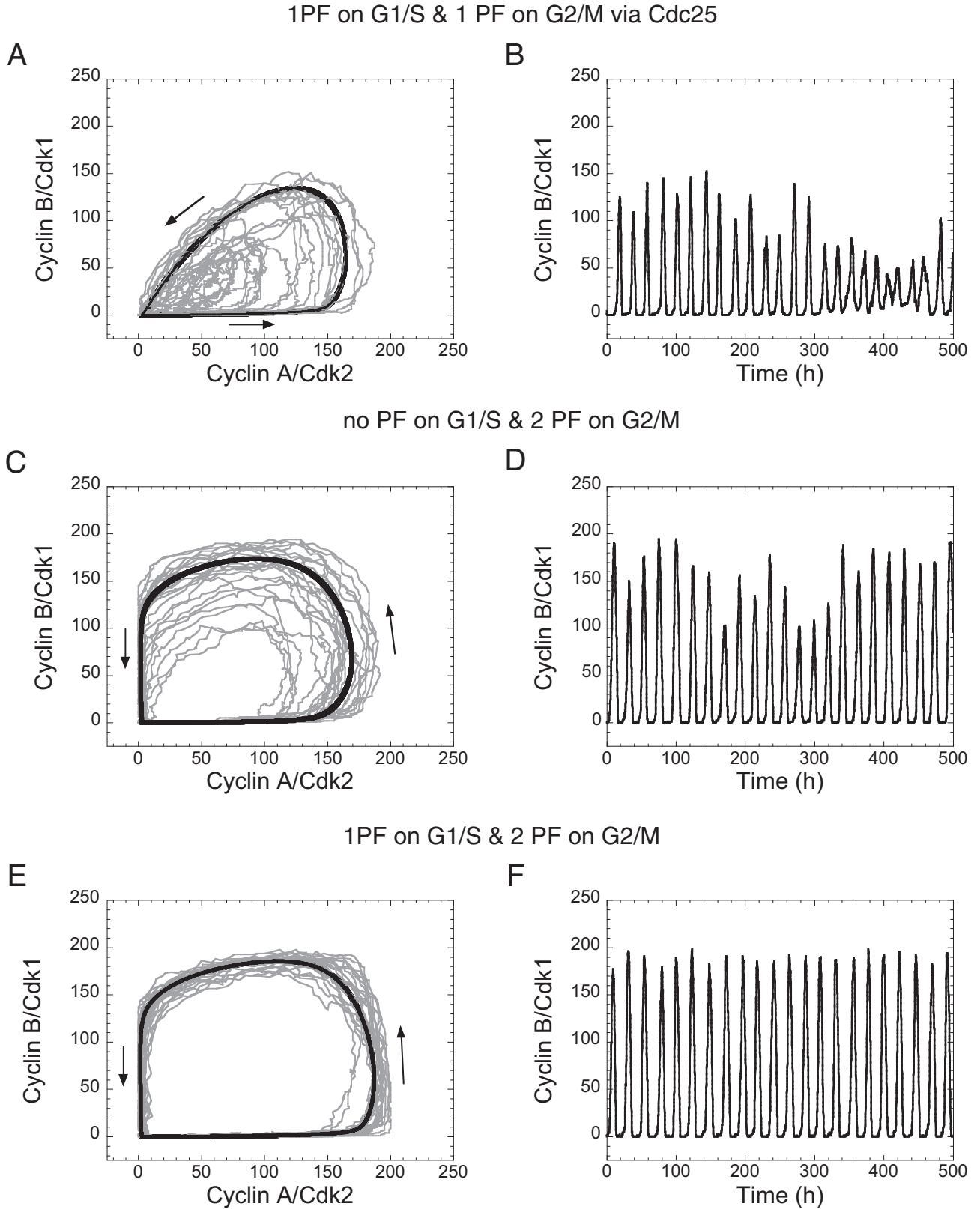
Note that at higher values of  $M_{\text{BTOT}}$ , cyclin B/Cdk1 does not reach full activity as a consequence of a large activation rate of Cdc20,  $V_{1\text{CDC}20}$ , which controls the rate of degradation of cyclin B/Cdk1 and cyclin A/Cdk2. In these conditions, cyclin B/Cdk1 strongly activates Cdc20, which in turn, rapidly promotes cyclin A/Cdk2 and cyclin B/Cdk1 degradation before cyclin B/Cdk1 reaches the upper stable steady state of the bistable switch. A decrease in  $V_{1\text{CDC}20}$  permits to increase the amplitude of cyclin B/Cdk1 (Fig. S1 in Supplementary Information).

The diminished regularity of Cdk oscillations when  $M_{\text{BTOT}}$  increases is further illustrated by the stochastic time evolution of cyclin B/Cdk1 (compare Fig. 7A with Figs. 7C, 7E). When  $M_{\text{BTOT}}$  increases the amplitude of cyclin B/Cdk1 oscillations and the cell cycle time are more irregular. Indeed, the coefficient of variation of the cell cycle times passes from 5% (for  $M_{\text{BTOT}} = 1$  in Fig. 7A, B) to 7.8% (for  $M_{\text{BTOT}} = 2$  in Fig. 7C, D) and 10.1% (for  $M_{\text{BTOT}} = 10$  in Fig. 7E, F).

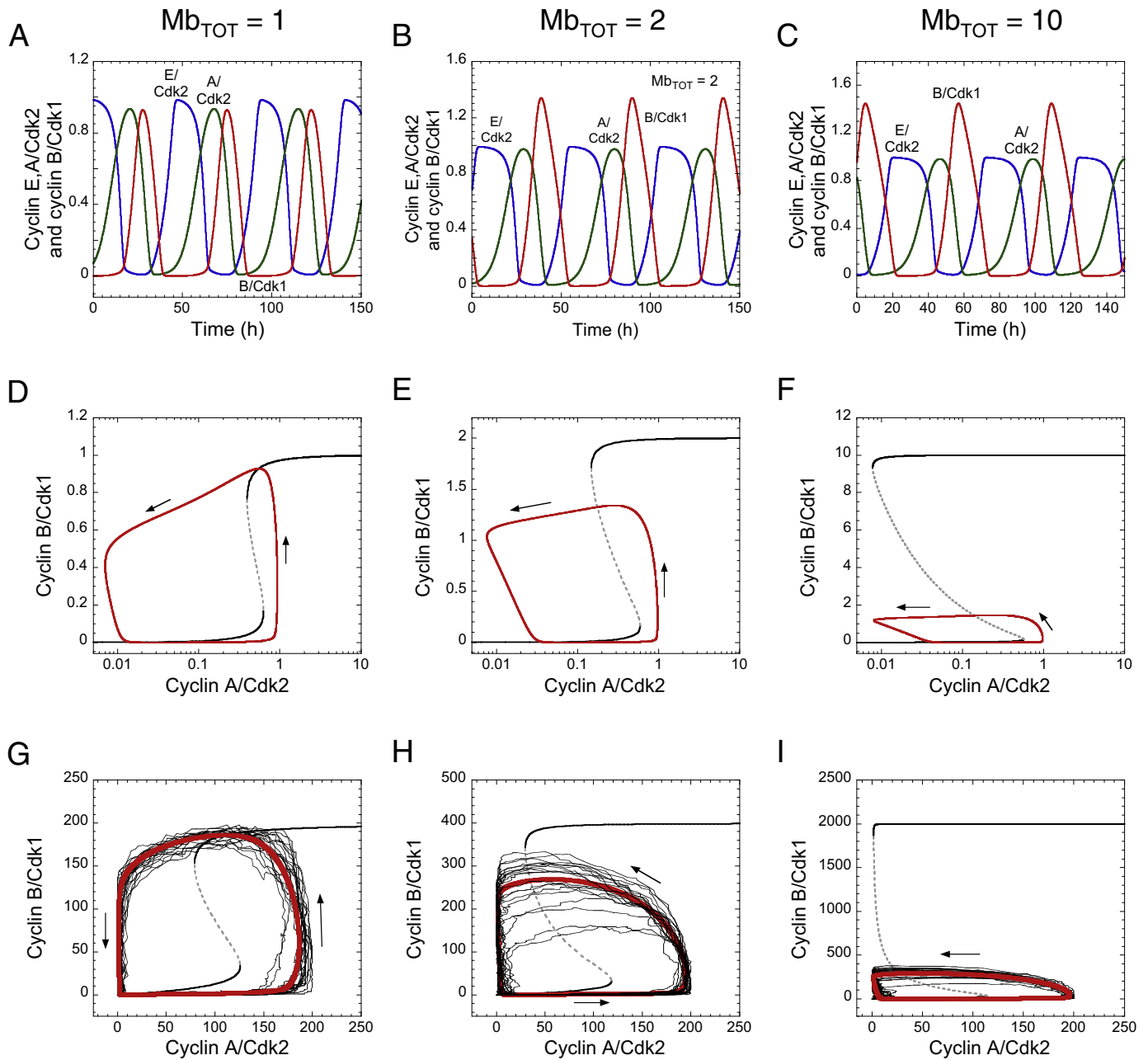
Thus, besides the importance of multiple, redundant, positive feedback loops for the robustness of Cdk oscillations, the model emphasizes the need of a proper balance in the expression of the various cyclin/Cdk complexes to ensure robust Cdk oscillations. A larger domain of bistability does not necessarily imply more robust Cdk oscillations if the system does not reach, during each oscillatory cycle, the two branches of the bistable switch.

## 6. Stochastic dynamics of the cell cycle in a cell population

In the previous section, we showed by means of a model developed for a single cell that the presence of PF loops at the core of cell cycle transitions and a proper level of cyclin/Cdk expression increase the robustness towards molecular noise of the dynamics underlying cell cycle transitions. We saw in Fig. 4B that the pres-



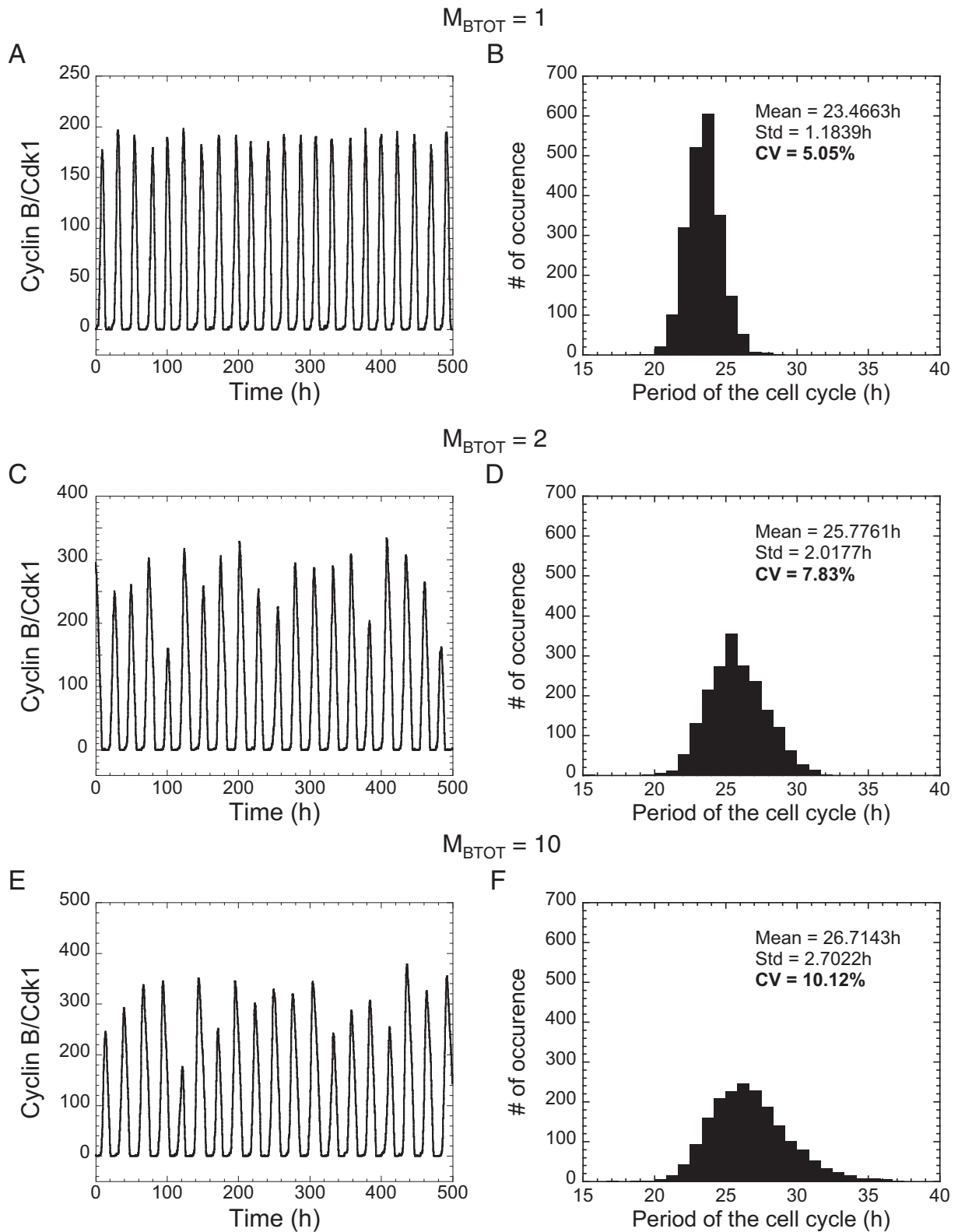
**Fig. 5.** PF loops increase the robustness of the oscillatory dynamics of the Cdk network. The deterministic (black curve) and the stochastic (grey curve) limit cycle trajectories of the Cdk network are illustrated in a phase plane defined by cyclin B/Cdk1 and cyclin A/Cdk2 in the presence of (A) 1 PF loop on G1/S ( $b_1 = 1$ ) and 1 PF loop on G2/M ( $b_2 = 1$ ), (C) of 2 PF loops on G2/M ( $b_2 = 1$  and  $K_{IB} = 0.5$ ), and (E) of 1 PF loop on G1/S ( $b_1 = 1$ ) and 2 PF loops on G2/M ( $b_2 = 1$  and  $K_{IB} = 0.5$ ). The corresponding stochastic temporal evolution of cyclin B/Cdk1 is illustrated in panels B, D and F, respectively. Other parameter values are as in Table S2 in Supplementary Information.



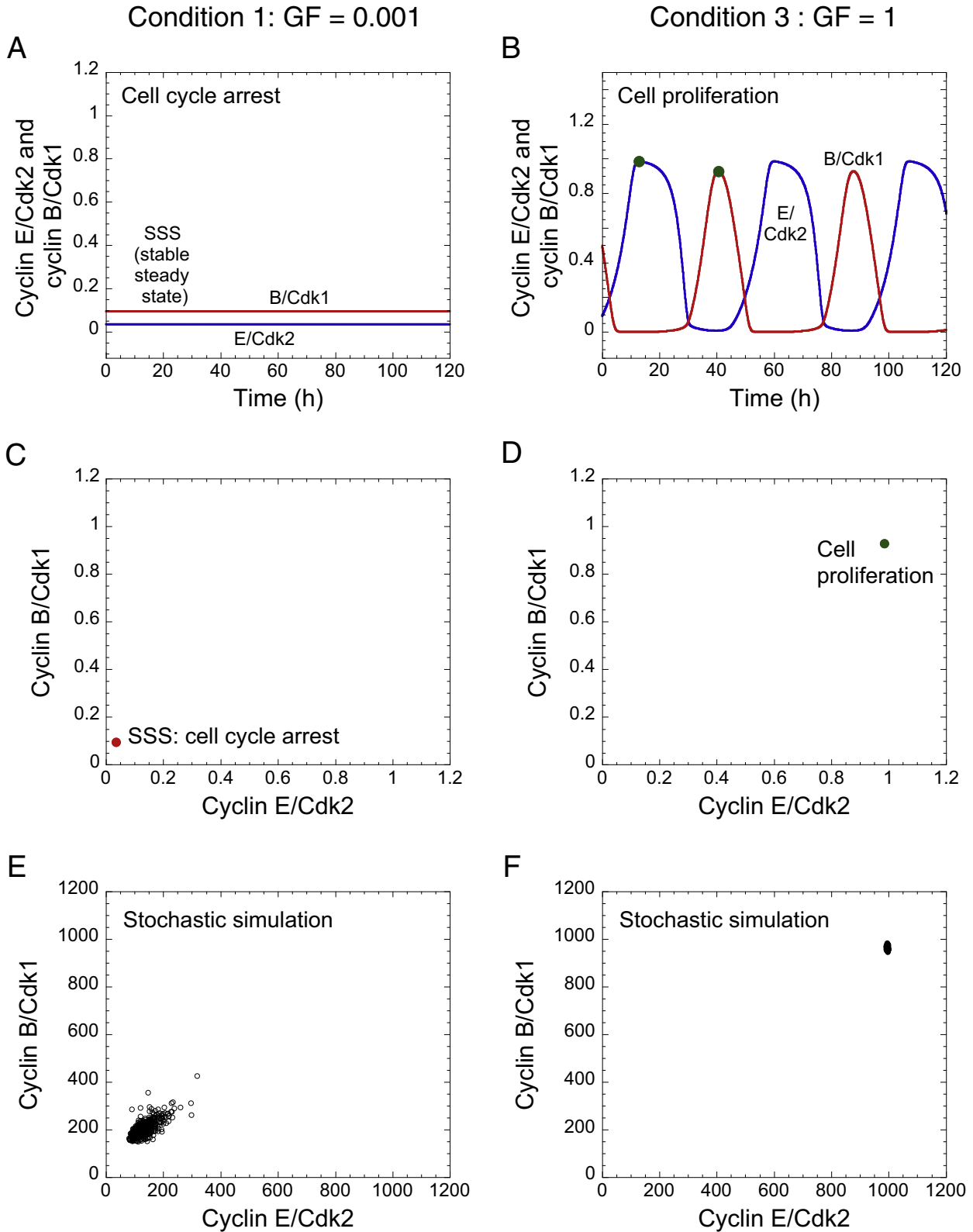
**Fig. 6.** Robustness of Cdk oscillations is affected by the total cyclin B/Cdk1 level,  $M_{BTOT}$ . Shown are the deterministic (A–F) and stochastic (G–I) simulations of the Cdk network in the presence of increasing levels of  $M_{BTOT}$  ( $M_{BTOT}=1$  in A, D, G;  $M_{BTOT}=2$  in B, E, H; and  $M_{BTOT}=10$  in C, F, I). (A–C) Deterministic temporal evolution of cyclin E/Cdk2, cyclin A/Cdk2 and cyclin B/Cdk1. (D–F) Steady-state levels of cyclin B/Cdk1 as a function of cyclin A/Cdk2, considered as an input parameter. The deterministic limit cycle trajectories in the cyclin A/Cdk2 versus cyclin B/Cdk1 phase plane are superimposed on the bifurcation diagrams (red curves). (G–I) Stochastic limit cycle trajectories (thin black curves) corresponding to the deterministic cases in D–F, respectively, are superimposed on the bifurcation diagrams. Other parameter values are as in Table S2.

ence of multiple PF loops creates, for intermediate levels of GF, a domain a coexistence between a stable steady state, associated with cell cycle arrest, and a regime of sustained oscillations corresponding to cell proliferation. The question arises as to whether molecular noise can trigger the switch from cell cycle arrest to cell proliferation, for a given set of parameter values? To explore this possibility, we performed deterministic and stochastic simulations of the model in the presence of 3 different levels of GF corresponding to conditions 1, 2, and 3 in Fig. 4B. As illustrated by the time evolution of cyclin E/Cdk and cyclin B/Cdk1, the model predicts the existence of a stable steady state of the Cdk network for low levels of GF (Fig. 8A where  $GF=0.001$ , condition 1 in Fig. 4B), while

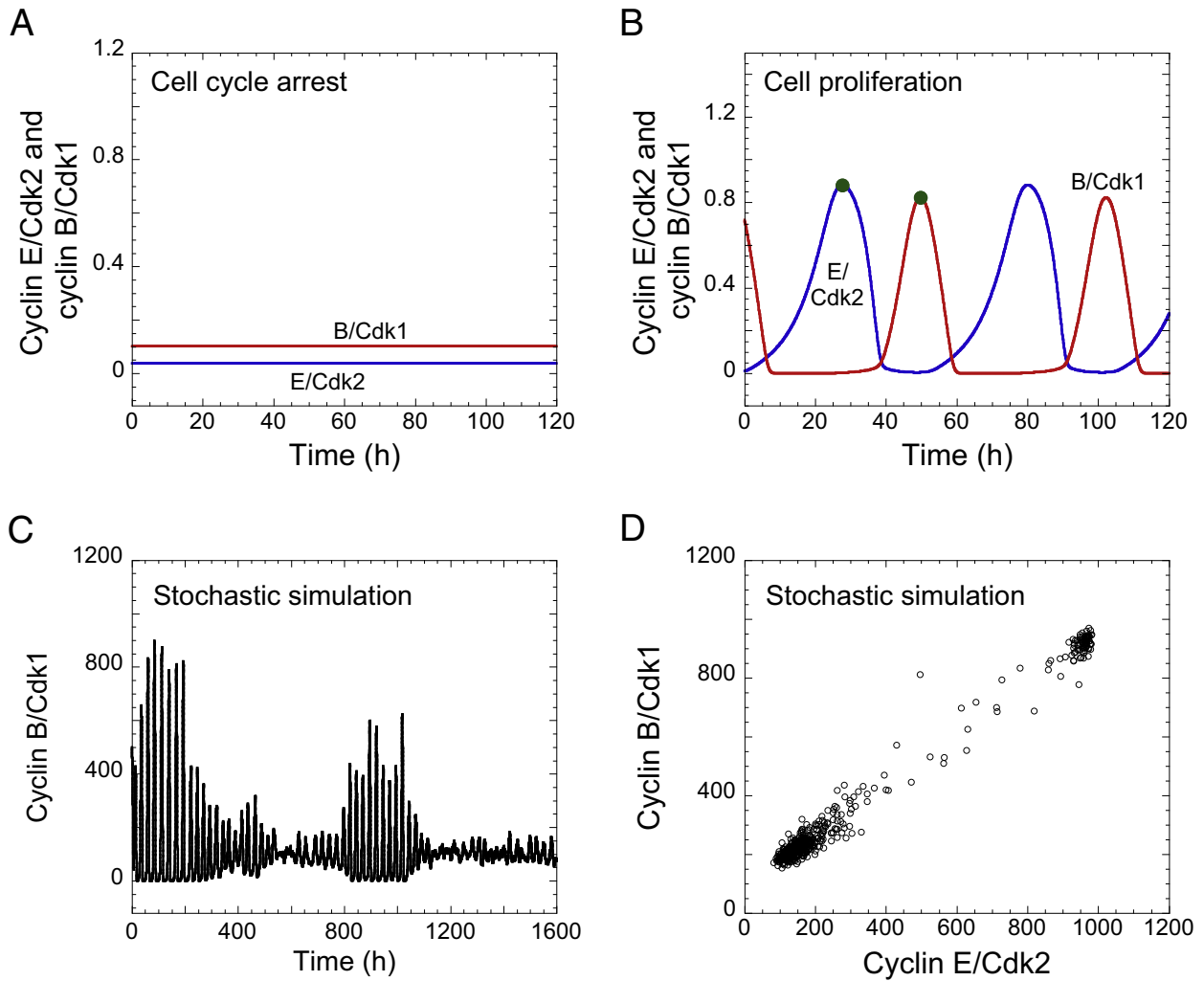
sustained oscillations of the cyclin/Cdk complexes occur for high levels of GF (Fig. 8B where  $GF=1$ , condition 3 in Fig. 4B) —we will examine the situation encountered at intermediate levels of GF further below. By plotting the maximum deterministic levels of cyclin E/Cdk2 and cyclin B/Cdk1 in the cyclin E/Cdk2 versus cyclin B/Cdk1 plane, the model illustrates that low expression levels of both cyclin/Cdk complexes correlate with cell cycle arrest (Fig. 8C) while high maximal levels correlate with cell proliferation (Fig. 8D). The corresponding stochastic simulations in a set of 500 versions of the same cellular stochastic model, corresponding to a population of 500 cells, indicate that both states, i.e. cell cycle arrest with low levels of GF, or active cell proliferation with high levels of GF, are



**Fig. 7.** Quantitative impact of cyclin B/Cdk1 levels on the robustness of oscillations in the skeleton model for the mammalian cell cycle. Stochastic temporal evolution of cyclin B/Cdk1 (A, C, E) and histograms of the corresponding period of the oscillations (B, D, F) are shown for  $M_{\text{BTOT}} = 1$  (A, B),  $M_{\text{BTOT}} = 2$  (C, D), and  $M_{\text{BTOT}} = 10$  (E, F). (A, C, E) Stochastic temporal evolution of cyclin B/Cdk1 correspond to the stochastic trajectories in Fig. 6 G-I, respectively. Other parameter values are as in Table S2 in Supplementary Information. (B, D, F) The coefficient of variation, CV, of the period of cyclin B/Cdk1 oscillations is of (B) 5.05% for  $M_{\text{BTOT}} = 1$ , (D) 7.83% for  $M_{\text{BTOT}} = 2$ , and (F) 10.12% for  $M_{\text{BTOT}} = 10$ .



**Fig. 8.** Cell cycle dynamics in single cells and cell populations at low and high levels of growth factor (GF). (A, B) Deterministic time evolution of cyclin E/Cdk2 and cyclin B/Cdk1, and (C, D) corresponding maximum levels of cyclin E/Cdk2 and cyclin B/Cdk1 are shown for GF=0.001 (A, C) and GF=1 (B, D). Conditions 1 (cell cycle arrest, GF=0.001) and 3 (cell proliferation, GF=1) correspond to the vertical lines in the bifurcation diagram in Fig. 4B. (E, F) The corresponding maximum levels of cyclin E/Cdk2 and cyclin B/Cdk1 are plotted in a stochastic cell population. Each circle corresponds to one of 500 cells, after 1000 h of transient evolution; parameter  $\Omega$  used in stochastic simulations is equal to 1000. (B) Green dots correspond to the maximum levels of cyclin E/Cdk2 and cyclin B/Cdk1 represented in (D). Other parameter values are as in Table S2. The results have been obtained by deterministic or stochastic simulations of the skeleton model for the mammalian cell cycle (see Supplementary Information).

Condition 2 :  $GF = 0.02$ 

**Fig. 9.** Effect of molecular noise on the balance between cell cycle arrest and cell proliferation. For intermediate value of  $GF$  ( $GF=0.02$  nM) and depending on initial conditions, the Cdk network, represented by the temporal evolution of cyclin E/Cdk2 and cyclin B/Cdk1, tends either to a stable steady state corresponding to cell cycle arrest (A), or to sustained oscillations corresponding to cell proliferation (B). The coexistence of a stable steady state with stable oscillations corresponds to the condition 2 in Fig. 4B (C) Stochastic time evolution of cyclin B/Cdk1, for  $GF=0.02$  and  $M_{BTOT}=1$ . (D) The maximum levels of cyclin E/Cdk2 and cyclin B/Cdk1 are plotted in a stochastic cell population. Each circle corresponds to one cell in a stochastic population of 500 cells, for  $\Omega=1000$ , after a transient of 1000 h. The initial conditions (IC) used to obtain in B a regime of Cdk oscillations associated with cell proliferation or used for stochastic simulations in D are:  $M_D = E2F = M_E = M_A = M_B = CDC20 = 0.5$  nM, while the IC used in A for reaching the steady state corresponding to cell cycle arrest are:  $M_D = E2F = M_E = M_A = M_B = CDC20 = 0.01$  nM. Other parameter values are as in Table S2.

highly robust with respect to random fluctuations (Figs. 8E and 8F where each circle represents one cell).

At intermediate values of  $GF$  (condition 2 in Fig. 4B, where  $GF=0.02$ ), depending on initial conditions, the Cdk network tends either to a stable steady state, corresponding to cell cycle arrest, or to a sustained oscillatory regime associated with cell proliferation (see the deterministic temporal evolution of cyclin E/Cdk2 and cyclin B/Cdk1 with 2 different sets of initial conditions in Figs. 9A and 9B). Turning to stochastic simulations, we observe that when a stable steady state coexists with a stable oscillatory regime, reversible stochastic switches between quiescence and proliferation may occur, as evidenced by the stochastic time evolution of cyclin B/Cdk1 (Fig. 9C). Interestingly, the corresponding stochastic simulations in a population of 500 cells, where all cells start from the same initial conditions, indicate that some cells reach a state of cell cycle arrest while others tend to a state of active cell proliferation

(Fig. 9D). This result shows that molecular noise can be a source of heterogeneity for the proliferative capacity in a cell population.

As illustrated in the bifurcation diagrams of Fig. 4D and 4F, high values of the total level of cyclin B/Cdk1,  $M_{BTOT}$ , favor a coexistence between a stable steady state and a sustained oscillatory regime even at low  $GF$  levels. Thus, in the presence of larger  $M_{BTOT}$  levels (e.g.,  $M_{BTOT}=2$ ), this dynamical property also permits to trigger heterogeneity in a stochastic cell population where some cells will tend to a state of cell cycle arrest while some cells will display active proliferation (condition 4 in Fig. 4D, where  $GF=0.001$ ). Since high levels of cyclin B/Cdk1 are a characteristic of cancer cells (Bednarek et al., 2016; Yang et al., 2016), the model suggests that the coexistence between distinct dynamical states of the cell cycle (arrest or proliferation) could be present in cancer cells and provide a source of heterogeneity in these cells. This is in line with the experimental observation that cancer cells are often defined by

a high level of heterogeneity (Gay et al., 2016; Gupta et al., 2011; McGranahan and Swanton, 2017).

## 7. Discussion

Numerous studies have emphasized the role of positive feedback loops and bistability in the dynamics of the cell cycle. This aspect has been addressed both in experiments and models for the early cell cycles in amphibian embryos (Ferrell and Machleder, 1998; Novak and Tyson, 1993; Pomerening et al., 2003; Pomerening et al., 2005; Sha et al., 2003; Tyson and Novak, 2001) and for the yeast cell cycle (Charvin et al., 2009; Chen et al., 2004; Dirick and Nasmyth, 1991; Sabouri-Ghomi et al., 2008). Thus the occurrence of bistability in Cdc2 activation as a function of cyclin B was predicted theoretically and verified experimentally in cell extracts of frog embryos (Pomerening et al., 2003; Sha et al., 2003). The capability of positive feedback loops to generate bistability, emphasized by René Thomas (Thomas, 1978; Thomas and d'Ari, 1990), was also stressed experimentally and theoretically for the mammalian cell cycle (Gérard and Goldbeter, 2009; Novak and Tyson, 2004; Skotheim et al., 2008; Yao et al., 2008).

After developing a detailed computational model for the Cdk network driving the mammalian cell cycle (Gérard and Goldbeter, 2009), containing 39 variables, we constructed reduced versions of this model containing only 5 variables (Gérard and Goldbeter, 2011). The latter skeleton model was then extended, without increase in the number of variables, by the addition of Cdk regulation through phosphorylation-dephosphorylation (Gérard and Goldbeter, 2011; Gérard et al., 2012). Both the detailed and skeleton models predict the occurrence of sustained Cdk oscillations in the presence of sufficient amounts of growth factor. These oscillations account for the sequential, transient, repetitive activation of the various cyclin/Cdk complexes that control the successive phases of the cell cycle (Fig. 2). Moreover, in both the detailed and the skeleton models, the regulatory structure, based on multiple negative feedback loops, allows for the occurrence of endoreplication (see Fig. 2E, F and (Gérard and Goldbeter, 2009; Gérard and Goldbeter, 2010)).

While the first version of the skeleton model allowed us to show that the regulatory wiring of the Cdk network can account for the temporal dynamics of the more comprehensive model containing additional biochemical details, the second version of the skeleton model incorporating Cdk regulation through phosphorylation-dephosphorylation allowed us to assess how the presence of positive feedback loops affects the robustness of oscillatory behavior in the Cdk network. Multiple PF loops are indeed involved in the regulation of cyclin E/Cdk2 and cyclin B/Cdk1 through phosphorylation-dephosphorylation (Fig. 1).

Bifurcation analyses of the G2/M module of the Cdk network show that the multiplicity of PF loops in this module centered on cyclin B/Cdk1 enlarges the domain of bistability when the steady-state level of cyclin B/Cdk1 is determined as a function of cyclin A/Cdk2 considered as a parameter —this procedure consists in isolating the Cdk1 module from the other modules of the Cdk network, and studying its dynamical properties as a function of its direct input, cyclin A/Cdk2 (Fig. 3 and (Gérard et al., 2012)). Such bistability phenomenon is crucial for the occurrence of an abrupt and irreversible G2/M transition. A similar increase of the bistability domain was previously noted in systems coupling two positive feedback loops (Chang et al., 2010; Domingo-Sananes and Novak, 2010; Ferrell, 2008). The model also shows that an increase in the total level of cyclin B/Cdk1 enlarges the magnitude of the bistable domain and the oscillatory domain of the Cdk network (Figs. 3 and 4). This result is in agreement with the fact that cancer cells are often characterized by overexpression of Cdk1 and by a high proliferative state.

By inducing bistability, PF loops not only promote the occurrence of Cdk oscillations of large amplitude but also enhance the robustness of Cdk oscillations towards molecular noise (Gérard et al., 2012). Here we revisited this property in further detail by comparing the deterministic and stochastic limit cycles trajectories in the presence of increasing number of PF loops characterizing the G1/S and G2/M transitions (Fig. 5) at different values of the total amount of cyclin B/Cdk1 (Fig. 6).

The results of Fig. 5 and our previous analysis (Gérard et al. 2012) show that the larger the domain of bistability, the stronger the resistance of Cdk oscillations with respect to molecular noise. This result can be explained as follows: once the system jumps to the upper branch of stable steady states, it will have a higher propensity to remain on it for a longer period of time in spite of fluctuations if the range of bistability is wide. In contrast, if this range is narrow, it will be easier for the system to fall back on the lower branch of steady states.

Potapova et al., (2011) showed that mitotic progression correlates with Cdk1 substrate phosphorylation and remains reversible until nuclear envelope breakdown; failure to complete mitosis is called mitotic collapse. In the presence of chemical inhibition of Wee1 and Cdc25, i.e. without PF loops, cells prematurely and reversibly enter into mitosis (Potapova et al., 2011). Here, the model shows that, in the absence of PF loops, cyclin B/Cdk1 oscillations are very noisy and characterized by smaller amplitude (Fig. 5B, D, F). If the amplitude of cyclin B/Cdk1 is smaller, we might expect a lower level of substrate phosphorylation, and thus an incomplete (or reversible) mitotic progression corresponding to mitotic collapse. A theoretical model accounting for mitotic collapse has previously been proposed (Tuck et al., 2013). These authors explain mitotic collapse by the concomitant inhibition of Wee1 and Cdc25.

However, a larger range of bistability does not suffice to confer robustness on oscillatory behavior. The results of Fig. 6 show indeed that another key factor is the distance between the two branches of stable steady states. If this distance is too large, the system may not reach the upper branch when it passes the cyclin A/Cdk2 value corresponding to the limit point beyond which the system starts its excursion toward the upper branch. When  $M_{\text{BTOT}}=1$  (Fig. 6G), the upper branch is reached, in contrast to what happens for  $M_{\text{BTOT}}=2$  (Fig. 6H) or 10 (Fig. 6I). As a consequence, in the latter two cases the buffering provided by the system's residence on the upper branch of the bistable switch does not occur, so that the resistance to noise is greatly reduced.

Although a rise in the level of cyclin B/Cdk1 enlarges the domain of bistability in the G2/M module of the Cdk network (Fig. 3), the results of Fig. 6 show that increasing the level of cyclin B/Cdk1 fails to improve the robustness of Cdk oscillations towards molecular noise (compare the first with the second and third columns in Fig. 6). Thus, as observed in cancer cells, large levels of Cdk1 may favor the oscillatory behavior of the Cdk network, which corresponds to active cell proliferation. However, the dynamics of cells possessing large amounts of Cdk1 may be less robust with respect to stochastic fluctuations, which may favor cell to cell heterogeneity in a population, as often observed in cancer cells.

Stochastic simulations of the cell cycle network applied to a cell population reveal another source of heterogeneity in the case of hard excitation, i.e. when the bifurcation diagrams established as a function of the level of growth factor, GF (Fig. 4B, D, F) indicate, at intermediate levels of GF, the coexistence of a stable steady state and a stable oscillatory regime for the same value of GF in the Cdk network. Then, molecular fluctuations could trigger a single cell to switch from active proliferation to cell cycle arrest and vice versa (Fig. 9C). In the same conditions, stochastic simulations of a cell population reveal a strong heterogeneity within the population, with some cells characterized by a state of cell cycle arrest and the others defined by a state of cell proliferation (Fig. 9D). A

similar distribution of cells in two distinct states corresponding to cell quiescence or proliferation was found in stochastic simulations of a Boolean model for the Cdk network (Stoll et al., 2012).

To verify experimentally if the quiescence/proliferation switch is characterized by hard excitation, a single cell experiment measuring the mRNA expression levels of the different cyclins and Cdks in a culture cell line dependent of GF to proliferate could be performed for different increasing and decreasing levels of GF. At low GF levels, nearly all cells should be in a quiescent phase characterized by low expression levels of the different cyclins and Cdks. At high levels of GF, nearly all cells should proliferate with high expression levels of cyclins and Cdks. However, at intermediate levels of GF, the heterogeneity in the expression of cyclins and Cdks should be larger because some cells would be quiescent while the others should proliferate. If hard excitation is present, the transition from quiescence to proliferation should occur at a different GF threshold than the reverse transition (Fig. 4B).

An additional prediction is the reduction of the robustness of the cyclin/Cdk oscillations in the presence of cyclin B/Cdk1 overexpression (see Fig. 7A, C, E). To quantify this prediction, we plotted the histograms of the period of cyclin B/Cdk1 (Mb) oscillations for  $Mb_{TOT} = 1, 2$  or  $10$  (Fig. 7B, D, F). The coefficient of variation (CV) of the period increases when  $Mb_{TOT}$  increases. This trend could be assessed by performing single cell experiments and recording the cell division times for various expression levels of cyclin B and/or Cdk1.

In the absence of hard excitation, stochastic simulations of a cell population show that the Cdk network robustly tends either to cell cycle arrest in the presence of low GF levels (Fig. 8E), or to oscillations associated with active cell proliferation in the presence of high GF levels (Fig. 8F).

Abrupt transitions between quiescence and proliferation based on bistable switches have been reported in numerous experimental and theoretical studies (Spencer et al., 2013; Yao, 2014; Yao et al., 2008; Yao et al., 2011). Similarly to what we observed in our models, stochastic switches could affect the dynamics of such transitions (Golubev, 2012; Lee et al., 2010). The presence of stochastic switches between different cell phenotypes confers added flexibility to a cell population, thus favoring its survival in a fluctuating environment (Acar et al., 2008). Similar phenomena could occur in mammalian cell populations, in view of the existence of multiple attractors in the complex network that underlies cell cycle regulation.

## Acknowledgments

This work was supported by the F.R.S.-FNRS (CDR grant no. 26027580, “Auto-organisation in cell signalling”).

We wish to dedicate this article to the memory of our colleague and friend, professor René Thomas. René was a true man of the Renaissance, whose interests ranged widely from genetics to theoretical biology, and from nonlinear science to astronomy—he loved observing the stars—and classical music—he enjoyed above all listening to the string quartets of Haydn, and devised a program for determining musical temperament. What was unique about René was his enthusiasm, his capacity to marvel at the beauty of a musical piece or of a strange attractor generated by computer simulations. It was a source of joy in itself to observe the exhilarating pleasure that René derived from scientific research, how close to biology or how abstract it could be. We will remember René Thomas for his key scientific contributions to molecular biology and the logical analysis of gene regulatory networks, his mathematical exploration of conditions for multistability, his quest for beauty which he pursued in science, music and life, his radiant smile and this unique sparkle constantly present in his eyes.

## Supplementary materials

Supplementary material associated with this article can be found, in the online version, at doi:10.1016/j.jtbi.2018.10.042.

## References

- Acar, M., Mettetal, J.T., van Oudenaarden, A., 2008. Stochastic switching as a survival strategy in fluctuating environments. *Nat. Genet.* 40, 471–475. doi:10.1038/ng.110.
- Barik, D., Baumann, W.T., Paul, M.R., Novak, B., Tyson, J.J., 2010. A model of yeast cell-cycle regulation based on multisite phosphorylation. *Mol. Syst. Biol.* 6, 405. doi:10.1038/msb.2010.55.
- Bednarek, K., Kiwerska, K., Szaumkessel, M., Bodnar, M., Kostrzewska-Poczekaj, M., Marszałek, A., Janiszewska, J., Bartochowska, A., Jackowska, J., Wierzbicka, M., Grenman, R., Szyfter, K., Gieffing, M., Jarmuz-Szymczak, M., 2016. Recurrent CDK1 overexpression in laryngeal squamous cell carcinoma. *Tumour Biol.* 37, 11115–11126. doi:10.1007/s13277-016-4991-4.
- Chang, D.E., Leung, S., Atkinson, M.R., Reifler, A., Forger, D., Ninfa, A.J., 2010. Building biological memory by linking positive feedback loops. *Proc. Natl. Acad. Sci. U S A* 107, 175–180. doi:10.1073/pnas.0908314107.
- Charvin, G., Cross, F.R., Siggia, E.D., 2009. Forced periodic expression of G1 cyclins phase-locks the budding yeast cell cycle. *Proc. Natl. Acad. Sci. U S A* 106, 6632–6637. doi:10.1073/pnas.0809227106.
- Chen, K.C., Calzone, L., Csikasz-Nagy, A., Cross, F.R., Novak, B., Tyson, J.J., 2004. Integrative analysis of cell cycle control in budding yeast. *Mol. Biol. Cell* 15, 3841–3862. doi:10.1091/mbc.E03-11-0794.
- Dirick, L., Nasmyth, K., 1991. Positive feedback in the activation of G1 cyclins in yeast. *Nature* 351, 754–757. doi:10.1038/351754a0.
- Domingo-Sananes, M.R., Novak, B., 2010. Different effects of redundant feedback loops on a bistable switch. *Chaos* 20, 045120. doi:10.1063/1.3526967.
- Edgar, B.A., Zielke, N., Gutierrez, C., 2014. Endocycles: a recurrent evolutionary innovation for post-mitotic cell growth. *Nat. Rev. Mol. Cell Biol.* 15, 197–210. doi:10.1038/nrm3756.
- Felix, M.A., Labbe, J.C., Doree, M., Hunt, T., Karsenti, E., 1990. Triggering of cyclin degradation in interphase extracts of amphibian eggs by cdc2 kinase. *Nature* 346, 379–382. doi:10.1038/346379a0.
- Ferrell Jr., J.E., 2008. Feedback regulation of opposing enzymes generates robust, all-or-none bistable responses. *Curr. Biol.* 18, R244–R245. doi:10.1016/j.cub.2008.02.035.
- Ferrell Jr., J.E., Machleder, E.M., 1998. The biochemical basis of an all-or-none cell fate switch in *Xenopus* oocytes. *Science* 280, 895–898.
- Ferrell Jr., J.E., Pomeroy, J.R., Kim, S.Y., Trunnell, N.B., Xiong, W., Huang, C.Y., Machleder, E.M., 2009. Simple, realistic models of complex biological processes: positive feedback and bistability in a cell fate switch and a cell cycle oscillator. *FEBS Lett.* 583, 3999–4005. doi:10.1016/j.febslet.2009.10.068.
- Gay, L., Baker, A.M., Graham, T.A., 2016. Tumour Cell Heterogeneity. *F1000Res* 5, doi:10.12688/f1000research.7210.1.
- Genric, G., Desdouets, C., 2014. Polyploidization in liver tissue. *Am. J. Pathol.* 184, 322–331. doi:10.1016/j.ajpath.2013.06.035.
- Gérard, C., Goldbeter, A., 2009. Temporal self-organization of the cyclin/Cdk network driving the mammalian cell cycle. *Proc. Natl. Acad. Sci. U S A* 106, 21643–21648. doi:10.1073/pnas.0903827106.
- Gérard, C., Goldbeter, A., 2010. From simple to complex patterns of oscillatory behavior in a model for the mammalian cell cycle containing multiple oscillatory circuits. *Chaos* 20, 045109. doi:10.1063/1.3527998.
- Gérard, C., Goldbeter, A., 2011. A skeleton model for the network of cyclin-dependent kinases driving the mammalian cell cycle. *Interface Focus* 1, 24–35. doi:10.1098/rsfs.2010.0008.
- Gérard, C., Goldbeter, A., 2014. The balance between cell cycle arrest and cell proliferation: control by the extracellular matrix and by contact inhibition. *Interface Focus* 4, 20130075. doi:10.1098/rsfs.2013.0075.
- Gérard, C., Gonze, D., Goldbeter, A., 2012. Effect of positive feedback loops on the robustness of oscillations in the network of cyclin-dependent kinases driving the mammalian cell cycle. *FEBS J* 279, 3411–3431. doi:10.1111/j.1742-4658.2012.08585.x.
- Gérard, C., Tyson, J.J., Coudreuse, D., Novak, B., 2015. Cell cycle control by a minimal Cdk network. *PLoS Comput Biol* 11, e1004056. doi:10.1371/journal.pcbi.1004056.
- Gillespie, D.T., 1977. Exact stochastic simulation of coupled chemical reactions. *J. Phys. Chem.* 81, 2340–2361. doi:10.1021/j100540a008.
- Goldbeter, A., 1991. A minimal cascade model for the mitotic oscillator involving cyclin and cdc2 kinase. *Proc. Natl. Acad. Sci. U S A* 88, 9107–9111.
- Goldbeter, A., 1993. Modeling the mitotic oscillator driving the cell division cycle. *Comments on Theoret. Biol.* 3, 75–107.
- Goldbeter, A., 1996. *Biochemical Oscillations and Cellular Rhythms*. Cambridge Univ. Press, Cambridge, UK.
- Golubev, A., 2012. Transition probability in cell proliferation, stochasticity in cell differentiation, and the restriction point of the cell cycle in one package. *Prog. Biophys. Mol. Biol.* 110, 87–96. doi:10.1016/j.pbiomolbio.2012.05.002.
- Gonze, D., Gérard, C., Wacquier, B., Woller, A., Tosenberger, A., Goldbeter, A., Dupont, G., 2018. Modeling-Based Investigation of the Effect of Noise in Cellular Systems. *Front Mol. Biosci.* 5, 34. doi:10.3389/fmolb.2018.00034.
- Gonze, D., Hafner, M., 2010. Positive feedbacks contribute to the robustness of the cell cycle with respect to molecular noise. In: Lévine, J., Müllhaupt, P. (Eds.).

- In: *Advances in the Theory of Control, Signals and Systems with Physical Modeling. Lecture Notes in Control and Information Sciences*, 407. Springer, Berlin, Heidelberg, pp. 283–295.
- Goustin, A.S., Leof, E.B., Shipley, G.D., Moses, H.L., 1986. Growth factors and cancer. *Cancer Res.* 46, 1015–1029.
- Gupta, P.B., Fillmore, C.M., Jiang, G., Shapira, S.D., Tao, K., Kuperwasser, C., Lander, E.S., 2011. Stochastic state transitions give rise to phenotypic equilibrium in populations of cancer cells. *Cell* 146, 633–644. doi:10.1016/j.cell.2011.07.026.
- Hanahan, D., Weinberg, R.A., 2011. Hallmarks of cancer: the next generation. *Cell* 144, 646–674. doi:10.1016/j.cell.2011.02.013.
- Harvey, S.L., Charlet, A., Haas, W., Gygi, S.P., Kellogg, D.R., 2005. Cdk1-dependent regulation of the mitotic inhibitor Wee1. *Cell* 122, 407–420. doi:10.1016/j.cell.2005.05.029.
- Harvey, S.L., Enciso, G., Dephoure, N., Gygi, S.P., Gunawardena, J., Kellogg, D.R., 2011. A phosphatase threshold sets the level of Cdk1 activity in early mitosis in budding yeast. *Mol. Biol. Cell* 22, 3595–3608. doi:10.1091/mbc.E11-04-0340.
- He, E., Kapuy, O., Oliveira, R.A., Uhlmann, F., Tyson, J.J., Novak, B., 2011. System-level feedbacks make the anaphase switch irreversible. *Proc. Natl. Acad. Sci. U S A* 108, 10016–10021. doi:10.1073/pnas.1102106108.
- Hoffmann, I., Clarke, P.R., Marcote, M.J., Karsenti, E., Draetta, G., 1993. Phosphorylation and activation of human cdc25-C by cdc2-cyclin B and its involvement in the self-amplification of MPF at mitosis. *EMBO J.* 12, 53–63.
- Holt, L.J., Krutchinsky, A.N., Morgan, D.O., 2008. Positive feedback sharpens the anaphase switch. *Nature* 454, 353–357. doi:10.1038/nature07050.
- Kapuy, O., He, E., Lopez-Aviles, S., Uhlmann, F., Tyson, J.J., Novak, B., 2009. System-level feedbacks control cell cycle progression. *FEBS Lett.* 583, 3992–3998. doi:10.1016/j.febslet.2009.08.023.
- Lee, T.J., Yao, G., Bennett, D.C., Nevins, J.R., You, L., 2010. Stochastic E2F activation and reconciliation of phenomenological cell-cycle models. *PLoS Biol.* 8. doi:10.1371/journal.pbio.1000488.
- McGranahan, N., Swanton, C., 2017. Clonal Heterogeneity and Tumor Evolution: Past, Present, and the Future. *Cell* 168, 613–628. doi:10.1016/j.cell.2017.01.018.
- Morgan, D.O., 1995. Principles of CDK regulation. *Nature* 374, 131–134. doi:10.1038/374131a0.
- Novak, B., Tyson, J.J., 1993. Numerical analysis of a comprehensive model of M-phase control in *Xenopus* oocyte extracts and intact embryos. *J. Cell Sci.* 106 (Pt 4), 1153–1168.
- Novak, B., Tyson, J.J., 1997. Modeling the control of DNA replication in fission yeast. *Proc Natl Acad Sci U S A* 94, 9147–9152.
- Novak, B., Tyson, J.J., 2004. A model for restriction point control of the mammalian cell cycle. *J. Theor. Biol.* 230, 563–579. doi:10.1016/j.jtbi.2004.04.039.
- Novak, B., Tyson, J.J., Gyorffy, B., Csikasz-Nagy, A., 2007. Irreversible cell-cycle transitions are due to systems-level feedback. *Nat Cell Biol.* 9, 724–728. doi:10.1038/ncb0707-724.
- Pomerening, J.R., Sontag, E.D., Ferrell Jr., J.E., 2003. Building a cell cycle oscillator: hysteresis and bistability in the activation of Cdc2. *Nat. Cell Biol.* 5, 346–351. doi:10.1038/ncb954.
- Pomerening, J.R., Kim, S.Y., Ferrell Jr., J.E., 2005. Systems-level dissection of the cell-cycle oscillator: bypassing positive feedback produces damped oscillations. *Cell* 122, 565–578. doi:10.1016/j.cell.2005.06.016.
- Potapova, T.A., Sivakumar, S., Flynn, J.N., Li, R., Gorbsky, G.J., 2011. Mitotic progression becomes irreversible in prometaphase and collapses when Wee1 and Cdc25 are inhibited. *Mol. Biol. Cell* 22, 1191–1206. doi:10.1091/mbc.E10-07-0599.
- Sabouri-Ghomi, M., Ciliberto, A., Kar, S., Novak, B., Tyson, J.J., 2008. Antagonism and bistability in protein interaction networks. *J. Theor. Biol.* 250, 209–218. doi:10.1016/j.jtbi.2007.09.001.
- Sha, W., Moore, J., Chen, K., Lassaletta, A.D., Yi, C.S., Tyson, J.J., Sible, J.C., 2003. Hysteresis drives cell-cycle transitions in *Xenopus laevis* egg extracts. *Proc. Natl. Acad. Sci. U S A* 100, 975–980. doi:10.1073/pnas.0235349100.
- Skotheim, J.M., Di Talia, S., Siggia, E.D., Cross, F.R., 2008. Positive feedback of G1 cyclins ensures coherent cell cycle entry. *Nature* 454, 291–296. doi:10.1038/nature07118.
- Spencer, S.L., Cappell, S.D., Tsai, F.C., Overton, K.W., Wang, C.L., Meyer, T., 2013. The proliferation-quiescence decision is controlled by a bifurcation in CDK2 activity at mitotic exit. *Cell* 155, 369–383. doi:10.1016/j.cell.2013.08.062.
- Stoll, G., Viara, E., Barillot, E., Calzone, L., 2012. Continuous time Boolean modeling for biological signaling: application of Gillespie algorithm. *BMC Syst Biol.* 6, 116.
- Swat, M., Kel, A., Herzog, H., 2004. Bifurcation analysis of the regulatory modules of the mammalian G1/S transition. *Bioinformatics* 20, 1506–1511. doi:10.1093/bioinformatics/bth110.
- Thomas, R., 1978. Logical analysis of systems comprising feedback loops. *J. Theor. Biol.* 73, 631–656.
- Thomas, R., d'Ari, R., 1990. *Biological feedback*. CRC Press, Boca Raton, FL.
- Thomas, R., Kaufman, M., 2001. Multistationarity, the basis of cell differentiation and memory. I. Structural conditions of multistationarity and other nontrivial behavior. *Chaos* 11, 170–179.
- Thomas, R., Thieffry, D., Kaufman, M., 1995. Dynamical behaviour of biological regulatory networks. I. Biological role of feedback loops and practical use of the concept of the loop-characteristic state. *Bull. Math. Biol.* 57, 247–276.
- Tsai, T.Y., Choi, Y.S., Ma, W., Pomerening, J.R., Tang, C., Ferrell Jr., J.E., 2008. Robust, tunable biological oscillations from interlinked positive and negative feedback loops. *Science* 321, 126–129. doi:10.1126/science.1156951.
- Tuck, C., Zhang, T., Potapova, T., Malumbres, M., Novak, B., 2013. Robust mitotic entry is ensured by a latching switch. *Biol. Open* 2, 924–931. doi:10.1242/bio.20135199.
- Tyson, J.J., 1991. Modeling the cell division cycle: cdc2 and cyclin interactions. *Proc. Natl. Acad. Sci. U S A* 88, 7328–7332.
- Tyson, J.J., Novak, B., 2001. Regulation of the eukaryotic cell cycle: molecular antagonism, hysteresis, and irreversible transitions. *J. Theor. Biol.* 210, 249–263. doi:10.1006/jtbi.2001.2293.
- Vinod, P.K., Zhou, X., Zhang, T., Mayer, T.U., Novak, B., 2013. The role of APC/C inhibitor Emi2/XErp1 in oscillatory dynamics of early embryonic cell cycles. *Biophys. Chem.* 177–178, 1–6. doi:10.1016/j.bpc.2013.03.002.
- Yang, W., Cho, H., Shin, H.Y., Chung, J.Y., Kang, E.S., Lee, E.J., Kim, J.H., 2016. Accumulation of cytoplasmic Cdk1 is associated with cancer growth and survival rate in epithelial ovarian cancer. *Oncotarget* 7, 49481–49497. doi:10.18632/oncotarget.10373.
- Yao, G., 2014. Modelling mammalian cellular quiescence. *Interface Focus* 4, 20130074. doi:10.1098/rsfs.2013.0074.
- Yao, G., Lee, T.J., Mori, S., Nevins, J.R., You, L., 2008. A bistable Rb-E2F switch underlies the restriction point. *Nat. Cell Biol.* 10, 476–482. doi:10.1038/ncb1711.
- Yao, G., Tan, C., West, M., Nevins, J.R., You, L., 2011. Origin of bistability underlying mammalian cell cycle entry. *Mol. Syst. Biol.* 7, 485. doi:10.1038/msb.2011.19.
- Zielke, N., Kim, K.J., Tran, V., Shibutani, S.T., Bravo, M.J., Nagarajan, S., van Straaten, M., Woods, B., von Dassow, G., Rottig, C., Lehner, C.F., Grewal, S.S., Duronio, R.J., Edgar, B.A., 2011. Control of *Drosophila* endocycles by E2F and CRL4(CDT2). *Nature* 480, 123–127. doi:10.1038/nature10579.